Competing orders in two-dimensional Bose-Fermi Mixtures

L. Mathey[1], S. -W. Tsai[2], and A. H. Castro Neto[3]

[1] *Physics Department, Harvard University, Cambridge, MA 02138*
[2] *Department of Physics, University of California, Riverside, CA 92521*
[3] *Department of Physics, Boston University, 590 Commonwealth Ave., Boston, MA 02215*

(Dated: February 6, 2008)

Using a functional renormalization group approach we study the zero temperature phase diagram of two-dimensional Bose-Fermi mixtures of ultra-cold atoms in optical lattices, in the limit when the velocity of bosonic condensate fluctuations are much larger than the Fermi velocity. For spin-1/2 fermions we obtain a phase diagram, which shows a competition of pairing phases of various orbital symmetry (s, p, and d) and antiferromagnetic order. We determine the value of the gaps of various phases close to half-filling, and identify subdominant orders as well as short-range fluctuations from the RG flow. For spinless fermions we find that p-wave pairing dominates the phase diagram.

Since the realization of the Mott insulator (MI) transition [1] in ultra-cold atom systems, there has been remarkable progress in 'engineering' many-body states in a well-defined and tunable environment, due to the advances in trapping and manipulating ultra-cold atoms in optical lattices [2, 3, 4]. Important achievements include the creation of fermionic superfluids [5], the realization of the Tonks-Girardeau gas [6] and of Luttinger liquids [7], and the observation of noise correlations [8]. One of the subjects of intense study recently has been mixtures of ultra-cold bosonic and fermionic atoms. Experiments include the condensation of molecules in mixtures of fermionic atoms [5], and the observation of instabilities in Bose-Fermi mixtures (BFM) [9]. Many other intriguing many-body phenomena have been proposed, such as the appearance of charge density wave order (CDW) [10], de-mixing transition [11], the formation of composite particles [12], and polaronic effects [13]. Mixtures of ultra-cold bosonic and fermionic atoms that are subjected to optical lattices, which confine the atoms to move on a 2D lattice, exhibit one of the most intriguing phenomena of condensed matter physics, the competition of orders in many-body systems, which is also observed in a variety of materials, such as high-T_c compounds [14] and Bechgaard salts [15]. To capture the properties of the many-body state of these systems presents a significant theoretical challenge.

In this paper we study these systems using a functional renormalization group (RG) approach introduced in the context of the stability of the Fermi liquid fixed point [16], and that has been extensively applied to interacting electrons on lattices in the last few years [17, 18], and has recently been extended to include retardation effects associated with the electron-phonon interaction [19, 20]. Contrary to mean-field and variational approaches [21], the RG approach includes corrections to the full four-point vertices in the flow equations, and therefore treats all types of order in an unbiased way. In this way we obtain the phase diagram and the values of the gaps of the different types of order. Furthermore, we can read off the subdominant orders and the short distance fluctuations from the RG analysis.

The fermionic atoms in the BFM considered here are prepared either as a mixture of two hyperfine states (which we treat in an isospin language), to create spin-1/2 fermions, or in a single hyperfine state to create spinless fermions. Fermionic atoms in different hyperfine states interact via short-range, i.e., on-site interaction, whereas spinless fermions are essentially non-interacting. Besides two-body contact interactions, density fluctuations in a condensate of bosonic atoms induce attractive finite-range interactions between fermions, with a length scale given by the coherence length of the condensate. The competition between these two types of interaction leads to the possibilities of many types of different instabilities and, hence, to a rich phase diagram, as we discuss here. In the laboratory, this system can be realized as a ^{40}K-^{87}Rb mixture in an optical lattice created by Nd:YAG lasers. The interaction between the different atomic species can be manipulated by either tuning the system close to a Feshbach resonance, or by using more than one optical lattice to trap the different types of atoms and to spatially shift these lattices with respect to each other.

Ultracold atoms in optical lattices are very accurately described by a Hubbard model. In the following we write the model for the case of spin-1/2 fermions. The case of spinless fermions can be immediately obtained from this by ignoring one of the spin states. For a mixture of one type of bosonic atom and two fermionic types that are SU(2) symmetric, the Hamiltonian is given by:

$$H = -t_f \sum_{\langle ij \rangle, s} f_{i,s}^\dagger f_{j,s} - t_b \sum_{\langle ij \rangle} b_i^\dagger b_j - \sum_i (\mu_f n_{f,i} + \mu_b n_{b,i})$$
$$+ \sum_i \left[U_{ff} n_{f,i,\uparrow} n_{f,i,\downarrow} + \frac{U_{bb}}{2} n_{b,i} n_{b,i} + U_{bf} n_{b,i} n_{f,i} \right], (1)$$

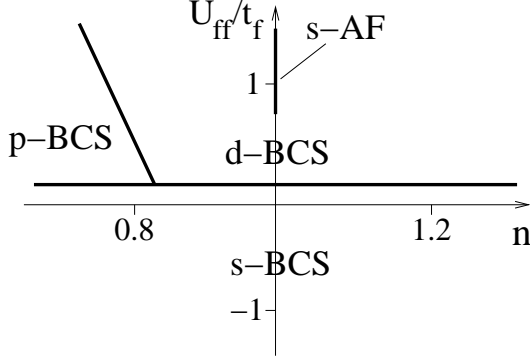where $f_{i,s}^\dagger$ ($f_{i,s}$) creates (annihilates) a fermion at site

FIG. 1: Phase diagram, interaction strength, U_{ff}/t_f, versus number of fermions per site, n, for a Fermi-Bose mixture in a square lattice in 2D ($\tilde{V}/t_f = 2$, $\xi = 1$).

i with pseudo-spin s ($s =\uparrow, \downarrow$), $b_i^\dagger$ (b_i) creates (annihilates) a boson at site i, $n_{f,i} = \sum_s f_{i,s}^\dagger f_{i,s}$ ($n_{b,i} = b_i^\dagger b_i$) is the fermion (boson) number operator, t_f and t_b are the fermionic and bosonic tunneling energies between neighboring sites, μ_f (μ_b) is the chemical potential for fermions (bosons), U_{bb} is the repulsion energy between bosons on the same site, U_{ff} is the interaction energy between the two species of fermions, and U_{bf} is the interaction energy between bosons and fermions. In momentum space, this Hamiltonian is written as:

$$H = \sum_{\mathbf{k}} \left\{ (\epsilon_{f,\mathbf{k}} - \mu_f) \sum_s f_{\mathbf{k},s}^\dagger f_{\mathbf{k},s} + (\epsilon_{b,\mathbf{k}} - \mu_b) b_{\mathbf{k}}^\dagger b_{\mathbf{k}} \right.$$
$$\left. + \frac{U_{ff}}{V} \rho_{f,\mathbf{k},\uparrow} \rho_{f,-\mathbf{k},\downarrow} + \frac{U_{bb}}{2V} \rho_{b,\mathbf{k}} \rho_{b,-\mathbf{k}} + \frac{U_{bf}}{V} \rho_{b,\mathbf{k}} \rho_{f,-\mathbf{k}} \right\} (2)$$

where $\rho_{f,\mathbf{k}} = \sum_{\mathbf{q},s} f_{\mathbf{k}+\mathbf{q},s}^\dagger f_{\mathbf{q},s}$ ($\rho_{b,\mathbf{k}} = \sum_{\mathbf{q}} b_{\mathbf{k}+\mathbf{q}}^\dagger b_{\mathbf{q}}$) is the fermion (boson) density operator, $\epsilon_{b/f,\mathbf{k}} = -2t_{b/f}(\cos k_x + \cos k_y)$, is the bosonic/fermionic dispersion relation for free particles on a square lattice.

Throughout this paper we consider the limit of weakly interacting bosons that form a BEC. We assume further that the velocity of the condensate fluctuations is much larger than the Fermi velocity. These two assumptions allow us to integrate out the bosonic degrees of freedom and use an instantaneous approximation, i.e. neglect retardation effects. In the limit of weakly interacting bosons, the following approach is well established: We assume that the zero momentum bosonic mode is macroscopically occupied, and we formally replace the corresponding operator b_0 by a real number $b_0 \rightarrow \sqrt{N_0}$, where N_0 is the number of condensed atoms. After this replacement we keep all terms that are quadratic in $b_{\mathbf{k}}$ (with $\mathbf{k} \neq 0$), and perform a Bogoliubov transformation, given by: $b_{\mathbf{k}} = u_{\mathbf{k}} \beta_{\mathbf{k}} + v_{\mathbf{k}} \beta_{-\mathbf{k}}^\dagger$, to diagonalize the bosonic Hamiltonian. The resulting eigenmodes $\beta_{\mathbf{k}}$ have a dispersion relation given by $\omega_{\mathbf{k}} = \sqrt{\epsilon_{b,\mathbf{k}}(\epsilon_{b,\mathbf{k}} + 2U_{bb}n_b)}$, with the low-$\mathbf{k}$ limit $\omega_{\mathbf{k}} \sim v_b|\mathbf{k}|$, with $v_b = \sqrt{2t_b U_{bb} n_b}$. The parameters $u_{\mathbf{k}}$ and $v_{\mathbf{k}}$ are given by: $u_{\mathbf{k}}^2 = (\omega_{\mathbf{k}} +$

$\epsilon_{b,\mathbf{k}} + U_{bb}n_b)/(2\omega_{\mathbf{k}})$ and $v_{\mathbf{k}}^2 = (-\omega_{\mathbf{k}} + \epsilon_{b,\mathbf{k}} + U_{bb}n_b)/(2\omega_{\mathbf{k}})$. The density fluctuations of the bosons are approximated by: $\rho_{b,\mathbf{k}} \approx \sqrt{N_0}(u_{\mathbf{k}} + v_{\mathbf{k}})(\beta_{\mathbf{k}} + \beta_{-\mathbf{k}}^\dagger)$, with $\mathbf{k} \neq 0$. The interaction between bosons and fermions is given by $U_{bf}\sqrt{N_0}/V \sum_{\mathbf{k}}(u_{\mathbf{k}} + v_{\mathbf{k}})(\beta_{\mathbf{k}} + \beta_{-\mathbf{k}}^\dagger)\rho_{f,-\mathbf{k}}$. As a next step we integrate out the bosonic modes and use an instantaneous approximation, leading to the following effective Hamiltonian:

$$H_{\text{eff.}} = \sum_{\mathbf{k}} \left\{ (\epsilon_{\mathbf{k}} - \mu_f) \sum_s f_{\mathbf{k},s}^\dagger f_{\mathbf{k},s} + \frac{U_{ff}}{V} \rho_{f,\mathbf{k},\uparrow} \rho_{f,-\mathbf{k},\downarrow} \right.$$
$$\left. + \frac{1}{2V} V_{\text{ind.},\mathbf{k}} \, \rho_{f,\mathbf{k}} \rho_{f,-\mathbf{k}} \right\}, \tag{3}$$

where the induced potential $V_{\text{ind.},\mathbf{k}}$ is given by: $V_{\text{ind.},\mathbf{k}} = -\tilde{V}/(1 + \xi^2(4 - 2\cos k_x - 2\cos k_y))$, with $\tilde{V}$ given by $\tilde{V} = U_{bf}^2/U_{bb}$, and ξ is the healing length of the BEC and is given by $\xi = \sqrt{t_b/2n_b U_{bb}}$. Notice, that this approach is only valid when $v_b \gg v_f$, so that the fermion-fermion interaction mediated by the bosons can be considered as instantaneous. In the presence of retardation one cannot formally define a Hamiltonian formulation since the frequency dependence of the interaction appears explicitly. If that is the case, one has to consider the frequency dependence of the interaction explicitly as is done, for instance, in ref. [19]. Here, however, the system can be tuned to the non-retarded limit, that is not the limit in most solid state systems.

Notice that (3) describes the scattering of two fermions from momenta $\mathbf{k}_1$ and $\mathbf{k}_2$, that are scattered into momenta $\mathbf{k}_3$ and $\mathbf{k}_4$. Momentum conservation at the interaction vertex requires that $\mathbf{k}_4 = \mathbf{k}_1 + \mathbf{k}_2 - \mathbf{k}_3$, and hence the interaction vertex, $U(\mathbf{k}_1, \mathbf{k}_2, \mathbf{k}_3)$, depends on three momenta [22]. Its bare value can be written as:

$$U(\mathbf{k}_1, \mathbf{k}_2, \mathbf{k}_3) = U_{ff} + V_{\text{ind.},\mathbf{k}_1 - \mathbf{k}_3}. \tag{4}$$

The RG is implemented by tracing out high energy degrees of freedom in a region between Λ and $\Lambda + d\Lambda$, where Λ is the energy cut-off of the problem. In this process, the vertex U is renormalized. At the initial value of the cut-off $\Lambda = \Lambda_0 \approx 8t_f$, the value of U is given by (4), which is the initial condition for the RG. The RG flow is obtained from a series of coupled integral-differential equations [17] for all the different interaction vertices $U(\mathbf{k}_1, \mathbf{k}_2, \mathbf{k}_3)$. From these, the specific interaction channels, such as CDW, antiferromagnetic (AF), and superconducting (BCS), can be identified:

$$V^{CDW} = 4\, U_c(\mathbf{k}_1, \mathbf{k}_2, \mathbf{k}_1 + \mathbf{Q}), \tag{5}$$
$$V^{AF} = 4\, U_\sigma(\mathbf{k}_1, \mathbf{k}_2, \mathbf{k}_1 + \mathbf{Q}), \tag{6}$$
$$V^{BCS} = U(\mathbf{k}_1, -\mathbf{k}_1, \mathbf{k}_2), \tag{7}$$

where we have use used: $U_c = (2 - \hat{X})U/4$, $U_\sigma = -\hat{X}U/4$ with $\hat{X}U(\mathbf{k}_1, \mathbf{k}_2, \mathbf{k}_3) = U(\mathbf{k}_2, \mathbf{k}_1, \mathbf{k}_3)$, and $\mathbf{Q}$ is the nesting vector, $\mathbf{Q} = (\pi, \pi)$. The RG equations read:

$$\partial_\ell U_\ell(\mathbf{k_1}, \mathbf{k_2}, \mathbf{k_3}) =$$

$$-\int_{p,\omega}\partial_\ell[G_\ell(\mathbf{p})G_\ell(\mathbf{k})]U_\ell(\mathbf{k_1},\mathbf{k_2},\mathbf{k})U_\ell(\mathbf{p},\mathbf{k},\mathbf{k_3})$$

$$-\int_{p,\omega}\partial_\ell[G_\ell(\mathbf{p})G_\ell(\mathbf{q_1})]U_\ell(\mathbf{p},\mathbf{k_2},\mathbf{q_1})U_\ell(\mathbf{k_1},\mathbf{q_1},\mathbf{k_3})$$

$$-\int_{p,\omega}\partial_\ell[G_\ell(\mathbf{p})G_\ell(\mathbf{q_2})]\left\{-2U_\ell(\mathbf{k_1},\mathbf{p},\mathbf{q_2})U_\ell(\mathbf{q_2},\mathbf{k_2},\mathbf{k_3})\right.$$

$$\left.+U_\ell(\mathbf{p},\mathbf{k_1},\mathbf{q_2})U_\ell(\mathbf{q_2},\mathbf{k_2},\mathbf{k_3})+U_\ell(\mathbf{k_1},\mathbf{p},\mathbf{q_2})U_\ell(\mathbf{k_2},\mathbf{q_2},\mathbf{k_3})\right\}(8)$$

where $\ell = \ln(\Lambda_0/\Lambda)$, $\mathbf{k} = \mathbf{k_1} + \mathbf{k_2} - \mathbf{p}$, $\mathbf{q_1} = \mathbf{p} + \mathbf{k_2} - \mathbf{k_3}$, $\mathbf{q_2} = \mathbf{p} + \mathbf{k_1} - \mathbf{k_3}$, and $G_\ell(\mathbf{k}) = \Theta(|\xi_{\mathbf{k}}| - \Lambda)/(i\omega - \xi_{\mathbf{k}})$ with $\xi_{\mathbf{k}} = \epsilon_{f,\mathbf{k}} - \mu_f$.

In our implementation we discretize the Fermi surface into $M = 24$ patches, and hence each of the interaction channels (5), (6), (7) is represented by an $M \times M$ matrix. At each RG step, we diagonalize each of these matrices. The channel with the largest eigenvalue (with the caveat that a BCS-channel needs to be attractive to drive a transition) corresponds to the dominant order. The elements of the eigenvector are labeled by the discrete patch indices around the Fermi surface and the symmetry of the order parameter is given by this angular dependence. In some parts of the phase diagram we encounter a divergence in the RG flow, indicating the onset of ordering with a gap that is in the detectable regime, i.e. larger than $10^{-3}t_f$. In other regimes, where such a divergence is not reached, one can read off the dominant tendency of the RG flow. In Fig. 2 we show examples of RG flows as a function of ℓ. In Fig. 2 (a), we show the competition between d-wave and s-wave pairing, with d-wave being dominant and s-wave being subdominant. In Fig. 2 (b) we show an example with dominant d-wave channel and subdominant AF channel. In both cases we find that for short distances (or high energies) CDW fluctuations are dominant, giving rise to a state that resembles the findings for high-T_c superconductors. Note that in some situations the many-body states are almost degenerate and small changes in the initial conditions (that is, changes in the form of the interactions) can be used to select one particular ground state.

With this procedure we determine the phase diagram of the system, which is shown in Fig. 1. We now discuss the general features of the phase diagram. In the absence of any coupling to the bosons, i.e. for $\tilde{V} = 0$, the system shows s-wave pairing for attractive interaction, $U_{ff} < 0$, and no ordering for $U_{ff} > 0$, i.e. Fermi liquid behavior, except for the special case of half-filling where Fermi surface nesting drives the system to AF order for repulsive interactions, and to s-wave pairing (degenerate with CDW) for attractive interaction. If we now turn on the interaction to the bosons, this picture is modified in the following way: The boundary of the s-wave regime is moved into the regime of positive U_{ff}, approximately to a value of U_{ff} where the effective interaction at the nesting vector $\mathbf{Q}$ between the fermions, $U_{ff} + V_{\text{ind.},\mathbf{Q}}$, is positive, i.e. for $U_{ff} \approx \tilde{V}/(1 + 8\xi^2)$. On the repulsive
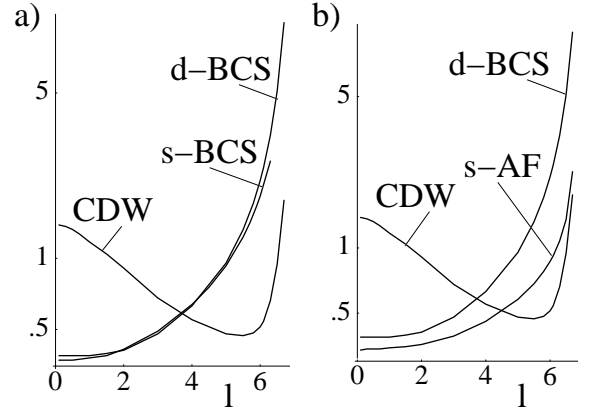

FIG. 2: RG flow for the different effective interactions (in units of t_f) as a function of the RG parameter l ($\tilde{V}/t_f = 3$ and $\xi = 1$). a) $U_{ff}/t_F = 0.5$; b) $U_{ff}/t_f = 1.2$.

side, and away from half-filling, we find the tendency to form a paired state, either d-wave or p-wave. This tendency becomes weaker the further the system is away from half-filling. We typically find a gap in the vicinity of half-filling and further away from $\mu = 0$ we find only an increasing strength of the corresponding interaction channel. For the half-filled system, we find that for attractive interactions the degeneracy between s-wave pairing and CDW ordering is lifted, with s-wave pairing being the remaining type of order. For repulsive interactions, we find an intermediate regime of d-wave pairing, and for larger values of U_{ff} we obtain AF order.

The RG approach also allows the extraction of the many-body gaps in the system through a "poor man's scaling" analysis of the divergent flow: at the point where the coupling becomes of order of t_f the scaling parameter ℓ reaches the maximum value $\ell^* = \ln(t_f/\Delta)$, where Δ is the value of the gap. Hence, $\Delta/t_f \approx \exp\{-\ell^*\}$ can be obtained from the RG flows such as the ones in Fig. 2. In Fig. 3 we show the gaps of the problem as a function of U_{ff}/t_f in the half-filled case. One can see that as U_{ff} increases, from negative to positive values, the s-wave gap is replaced by a d-wave gap, and finally for an antiferromagnetic gap. As is apparent from this figure, the gap in the d-wave phase is much smaller than the gaps of the AF order and the s-wave pairing, and, furthermore, almost independent of the value of U_{ff}. The latter is the case because the U_{ff} term is a pure s-wave contribution to the interaction and therefore does not contribute to the d-wave channel. The d-wave channel has an initial contribution which is entirely due to the anisotropy of the induced interaction, which gives only a small value, and as a consequence only a small value for the gap. The value of the gap (in units of t_f) can be numerically fitted with a BCS expression of the form $a\exp(-b/\tilde{V})$, with parameters a and b given by $a = 0.31$ and $b = 14.2$.
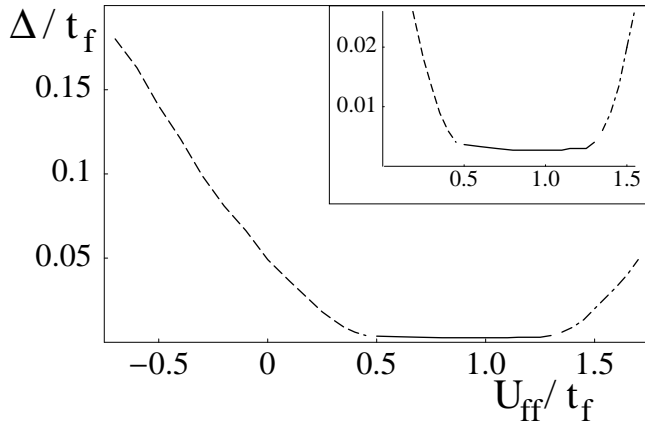
We have also performed RG calculations for a system

FIG. 3: Many-body energy gaps at half-filling ($\mu = 0$), as a function of U_{ff}/t_f, for $\tilde{V}/t_f = 3$ and at a fixed value of the coherence length $\xi = 1$. Dashed line: s-wave gap; Continuous line: d-wave gap; Dotted-dashed line: antiferromagnetic gap. The inset shows a magnified plot of the d-wave regime.

of spinless fermions. This can be obtained by suppressing one of the spin indices in (1) or (2). In this case there is a major simplification in the problem since U_{ff} is absent: in a spinless problem there can be only one fermion per site, as per Pauli's principle. Hence, in the absence of bosons, the spinless gas is non-interacting. The bosons, however, mediate the interaction between the fermions. Since the fermions are in different lattice sites the pair wavefunction has necessarily a node and hence, no s-wave pairing is allowed. In other words, in the spinless case the anti-symmetry of the wavefunction requires pairing in an odd angular momentum channel. In fact, we find that throughout the entire phase diagram the fermions develop p-wave pairing. At half-filling we find a similar behavior of CDW fluctuations on short scales, analogous to the flow shown in Fig. 2. One should point out that in real solids the conditions of "spinlessness" behavior is hard to achieve since it usually requires complete polarization of the electron gas, that is, magnetic energies of the order of the Fermi energy (a situation experimentally difficult to achieve in good metals). However, in cold atom lattices this situation can be easily accomplished with the correct choice of atoms.

The many-body states discussed in this paper can be observed through various methods: AF order could be revealed in time-of-flight images and Bragg scattering [23], noise correlations [8] can be used to detect the various pairing phases, laser stirring experiments [24] can be used to detect the phase boundary between AF order and pairing. The short-scale CDW fluctuations should give a signature in a photo-association measurement. RF spectroscopy [25] can be used to quantify the gaps of the various phases.

In summary, we have used a functional RG approach to study BFM of ultra-cold atoms in a 2D optical lattice.

We found a number of competing phases, in particular in the vicinity of half-filling, including AF ordering, s-, p-, and d-wave pairing. Our approach enables us to quantify the gaps of these phases, to identify subdominant orders, and to study short-range fluctuations. Optical lattices of cold atoms allow for a unique opportunity of study of complex many-body states under well controlled circumstances, a situation that can be hardly found in real solids.

[1] M. Greiner, *et al.*, Nature (London) **415**, 39 (2002).
[2] T. Stöferle, *et al.*, Phys. Rev. Lett. **92**, 130403 (2004).
[3] O. Mandel, *et al.*, Phys. Rev. Lett. **91**, 010407 (2003); O. Mandel, *et al.*, Nature (London) **425**, 937 (2003).
[4] M. Koehl, *et al.*, cond-mat/0410389.
[5] M. Greiner, *et al.*, Nature **426**, 537 (2003); S. Jochim, *et al.*, Science **302**, 2101 (2003); M.W. Zwierlein, *et al.*, Phys. Rev. Lett. **91**, 250401 (2003).
[6] B. Paredes, *et al.*, Nature **429**, 277 (2004).
[7] H. Moritz, *et al.*, Phys. Rev. Lett. **94**, 210401 (2005).
[8] M. Greiner, *et al.*, Phys. Rev. Lett. **94**, 110401 (2005); S. Foelling, *et al.* Nature **434**, 481-484 (2005); E. Altman, *et al.*, Phys. Rev. A **70**, 013603 (2004); L. Mathey, *et al.*, cond-mat/0507108.
[9] G. Modugno, *et al.*, Science, **297**, 2240 (2002); J. Goldwin, *et al.*, Phys. Rev. A **70**, 021601 (2004).
[10] R. Roth and K. Burnett, cond-mat/0310114; T. Miyakawa, et al., cond-mat/0401107; H.P. Büchler and G. Blatter, Phys. Rev. Lett. **91**, 130404 (2004); cond-mat/0402432.
[11] P. Sengupta and L. P. Pryadko, cond-mat/0512241.
[12] M.Y. Kagan, et al., cond-mat/0209481; M. Lewenstein, *et al.*, Phys. Rev. Lett. **92**, 050401 (2004); H. Fehrmann, *et al.*, cond-mat/0307635.
[13] L. Mathey, *et al.*, Phys. Rev. Lett. **93**, 120404 (2004); L. Mathey, and D.-W. Wang, in preparation.
[14] D. J. van Harlingen, Rev. Mod. Phys. **67**, 515 (1995).
[15] *Organic Conductors: Fundamentals and Applications*, ed. by J.P. Farges (Marcel Dekker, 1994).
[16] R. Shankar, Rev. Mod. Phys. **68**, 129 (1994).
[17] D. Zanchi and H.J. Schulz, Phys. Rev B **61**, 13609 (2000).
[18] C. J. Halboth and W. Metzner, Phys. Rev. B **61**, 7364 (2000); S.-W. Tsai and J. B. Marston, Can. J. Phys. **79** 1463 (2001); C. Honerkamp, cond-mat/0411267.
[19] S.-W. Tsai *et al.*, Phys. Rev. B **72**, 054531 (2005); *ibid.*, cond-mat/0505426.
[20] C. Honerkamp, and M. Salmhofer, Prog. Theor. Phys. **113**, 1145 (2005).
[21] D.-W. Wang, *et al.*, Phys. Rev. A **72**, 051604 (2005).
[22] $U(\mathbf{k}_1, \mathbf{k}_2, \mathbf{k}_3)$ denotes processes involving electrons with opposite spins. Processe involving parallel spins can be obtained from these [17].
[23] J.Stenger, *et al.*, Phys. Rev. Lett. **82**, 4569 (1999).
[24] C. Raman, *et. al.*, Phys. Rev. Lett. **83**, 2502 (1999); R. Onofrio, *et. al.*, Phys. Rev. Lett. **85**, 2228 (1999).
[25] C. Chin, *et al.*, Science **305**, 1128 (2004).